

Tweezers Manipulation Using High-speed Visual Servoing Based on Contact Analysis

Taku Senoo, Daiki Yoneyama, Akio Namiki and Masatoshi Ishikawa

Abstract—In this paper, the task of tweezers manipulation is considered with the goal of achieving dexterous manipulation of a human tool. First we analyze the contact state between fingers and tweezers in order to design preferable fingers for tool manipulation. Next the control method based on high-speed visual servoing is presented. Experimental results are shown in which a high-speed hand grasps a tiny grain with tweezers in 2-D and 3-D situations.

I. INTRODUCTION

Recently technologies integrating robots into society have been actively developed. However there still remain issues to be solved in regard to the adoption of robots into real society. One of the issues is adaptation to the environment which is optimally-designed for human beings. It is desirable for robots to act flexibly in the current environment only with minimal modification. In terms of mobility capability, bipedal robots provide one solution for moving around easily on uneven floor surface. Similarly it is effective for a single manipulator to handle various tools in situations where many types of tasks are required. In particular the use of industrial tools with specific functions for each task promotes the efficiency and diversification of robotic work.

A human can easily operate many types of tools much like extensions of his body. Tool manipulation should help us to understand why a human hand is so dexterous and what kinds of characteristics are required to develop skillful robot hands. There is much research regarding brain activity or its model during tool use. Iriki et al. have reported that the receptive fields of bimodal neurons that code the schema of the hand were modified to include the length of a tool through experiments with macaque monkeys [1]. This means that a tool can be an extension of the hand in both a physical and a functional sense. Nabeshima et al. have proposed a computational model for tool-body assimilation and verified by numerical simulation that a robot can grasp a target by touch with a tool in blind conditions [2].

On the other hand there is much research regarding recognition of tools focused on the relation between its shape and function [3], [4], [5], [6]. While some of them extend to the calculation of hand configuration for grasping tools, they have not been verified by actual experiments using a robotic hand.

T. Senoo, D. Yoneyama and M. Ishikawa are with Dept. of Creative Informatics, Graduate School of Information Science and Technology, University of Tokyo, 7-3-1 Hongo, Bunkyo-ku, Tokyo 113-8656, Japan. Taku.Senoo@ipc.i.u-tokyo.ac.jp

A. Namiki is with Dept. of Mechanical Engineering, Graduate School of Engineering, Chiba University, 1-33 Yayoi-cho Inage-ku Chiba-shi, Chiba 263-8522, Japan.

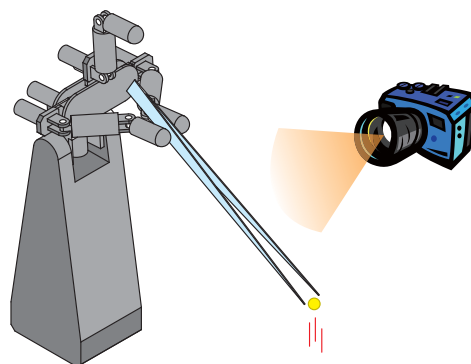


Fig. 1. Tweezers manipulation

As for practical robot manipulation using a tool, there has not been much research. Sugiuchi et al. have studied manipulation of scissors by a dual multi-finger hand arm system [7]. Kawasaki et al. have developed a haptic interface to manipulate plural tool devices for their multifingered hand [8]. Bernardin et al. have developed a tool manipulation system based on a human skill using a sensor fusion approach [9]. In this research, however, the tool is fixed to the end-effector with holding parts in order to simplify control. Therefore these are same kind of industrial robots which can achieve specialized operation with specific end-effector such as arc welding or spot welding. The current situation of tool manipulation is far from ideal because the dynamic property of contact state has not been actively used.

Based on this background, Mizusawa et al. have achieved grasping a tiny grain using tweezers as an example of tool manipulation [10]. In the previous paper, they treated the static case where the target was placed on a table. This task has been executed by high-speed visual servoing control of the contact state between fingers and tweezers. In this paper, we analyze the elastic contact state in order to design soft fingers for tool manipulation. In addition we have extended the range of application to 2-D and 3-D situations where the target moves on a plane and the target is shot in the air, respectively, as shown in Fig.1.

II. CONTACT ANALYSIS

A. Passive Joint

In tool manipulation, both robot hand and tool are considered as an assimilation system. In this case, it is difficult to control the state of the contact point between fingers and a tool because there is no actuator and its state has to be controlled by an indirect force acting there. Therefore

TABLE I
CONDITIONS OF CONTACT STATE

soft-finger contact	$\max\left(\frac{F_t}{\mu_{ts}}, \frac{M_n}{\mu_{rs}}\right) < F_n$
point contact	$\frac{F_t}{\mu_{ts}} < F_n < \frac{M_n}{\mu_{rs}}$
sliding contact	otherwise

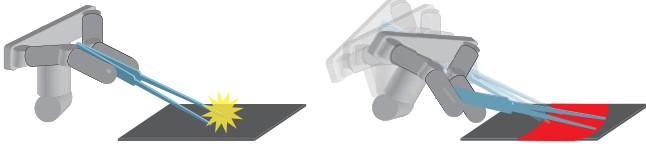


Fig. 2. Characteristics of contact using passive joint

Mizusawa defined the contact point as a “passive joint [10].” In a passive joint, there generally exists three contact phases; soft-finger contact, point contact and sliding contact. The contact phase is determined by the relationship between the force and the rotational moment.

In soft-finger contact, a tool is fixed to the fingers, and there is no change of the relative position and posture at the passive joint due to the rotational friction moment. In point contact, a tool can rotate around the passive joint while keeping the relative position constant. In sliding contact, a tool slides on the finger and the relative position at the passive joint changes. That is, a passive joint is a peculiar one whose type (prismatic joint or rotational joint) and structure (translation or direction of axis) can be changed depending on how the tool is to be grasped.

Let us consider the relationship between the force and the rotational moment. We assume that the tangential frictional force and the rotational moment around normal direction at contact point are approximated as the coulomb friction model and both have no effect each other. When a force, whose tangential component is F_t and normal component is F_n , is exerted at a passive joint, the frictional force F_f is described as

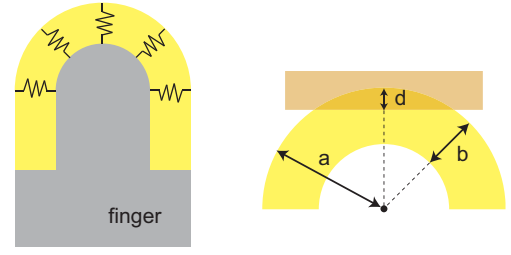
$$F_f = \begin{cases} F_t & (F_t < \mu_{ts}F_n) \\ \mu_{td}F_n & (F_t > \mu_{ts}F_n) \end{cases}, \quad (1)$$

where μ_{ts} and μ_{td} are coefficients of static and dynamic translational friction respectively. The rotational frictional moment M_f is similarly described as

$$M_f = \begin{cases} M_n & (M_n < \mu_{rs}F_n) \\ \mu_{rd}F_n & (M_n > \mu_{rs}F_n) \end{cases}, \quad (2)$$

where M_n is a normal component of the moment acting at a passive joint and μ_{rs} and μ_{rd} are coefficients of static and dynamic rotational friction respectively. Using Eqs.(1) and (2), the conditions of the contact state are calculated as shown in Table I.

With proper setting of force or moment acting at a passive joint, various motion such as the following can be achieved: impact motion for applying strong force, dragging surface



(a) Radially distributed model (b) Deformation

Fig. 3. Flexible finger model



Fig. 4. Developed fingers

using mainly the gravity effect, and transitional motion between contact states as shown in Fig.2.

B. Flexible Finger Structure

Generation of a certain level of rotational frictional moment is required to maintain soft-finger contact. Therefore, it is difficult to achieve the state between rigid bodies due to the low value of the coefficient of rotational friction. Here we discuss a robot finger covered with elastic skin to handle various states including soft-finger contact. We adopt hemisphere-shaped fingertip because it is possible to drastically change the hand configuration while keeping the posture of a tool in absolute coordinate space.

To examine the characteristics of flexible fingers, let us consider the contact model between a finger and rigid plane. We assume that finger skin consists of isotropic elastic elements which are radially distributed as shown in Fig.3. The tangential force due to deformation is totally zero because of reflective symmetry around the center on contact area. When the deformation amount is d , the normal force acting on contact area dF is represented by Hooke’s law as

$$dF = dK(a - \sqrt{r^2 + (a - d)^2}) \frac{a - d}{\sqrt{r^2 + (a - d)^2}}, \quad (3)$$

where dK is the spring constant, a is radius of the finger and b is the thickness of the elastic skin, respectively. The spring constant dK is represented using Young’s modulus E as

$$dK = \frac{EdS}{b} = \frac{E2\pi r dr}{b}, \quad (4)$$

where dS is the cross-sectional area of the spring and r is the distance from the center of contact area. The normal force

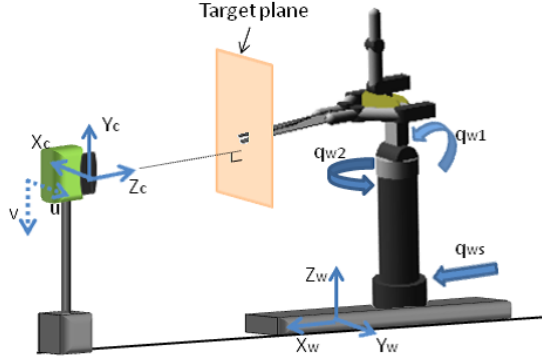


Fig. 5. Setting of coordinate system

F is calculated by integrating on the whole contact area as

$$\begin{aligned} F &= \frac{E 2\pi}{b} \int (a - \sqrt{r^2 + (a-d)^2}) \frac{a-d}{\sqrt{r^2 + (a-d)^2}} r dr \\ &= E\pi \frac{(a-d)d^2}{b}. \end{aligned} \quad (5)$$

In addition, the following constraint regarding the radius of the finger, thickness of elastic skin and the deformation is satisfied;

$$a > b > d. \quad (6)$$

The deformation and the contact area become large when Young's modulus is small, the radius of the finger is large and the thickness of elastic skin is large. In these cases, the coefficient of rotational friction becomes large and the contact state has the tendency to be in soft-finger contact or point contact. However too small Young's modulus or too large thickness of elastic skin introduces error in the tangential direction and leads to poor grasping performance because deviation from the contact model is increased. Based on the results, we have developed various types of fingers with the elastic skin as shown in Fig 4.

III. TWEEZERS MANIPULATION

We set grasping motion of a tiny grain using tweezers as the goal of the tool manipulation task. The hand is controlled to grasp the object in following three cases:

- (i) sliding object on a plane surface
- (ii) upward moving object in the air
- (iii) downward moving object in the air.

The object is so small and light that it hardly affects the dynamics of the hand and tweezers even at the moment of grasping. Therefore, we produce a strategy ignoring contact dynamics between tweezers and the object.

A. Grasping Strategy

In tool manipulation there exist two controlled objects, a tool controlled by fingers and a target controlled by a tool. Therefore, it is difficult to ensure a sufficient estimate of the accuracy of the state of controlled objects only using force sensors attached on fingers. In addition, the geometric information about a tool is very important for planning hand

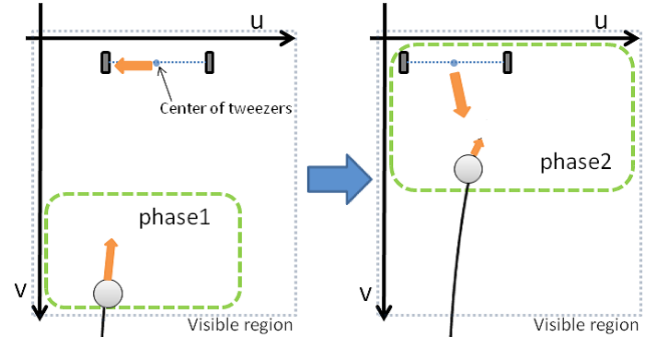


Fig. 6. Grasping motion for moving object in the air

motion based on kinematics of the assimilation system. In this case, an external vision sensor is particularly useful for detecting information about the objects directly, and smooth control can be executed with a high feedback rate of visual information. As a result, we introduce a high-speed vision system in order to achieve robust feedback control of a passive joint.

As a control method, we apply image-based visual servoing, which is based on feedback information about position error in the image plane. This method is robust against calibration error, and there is no need to compute the 3-D position of the object. In particular, this method has an advantage in tool manipulation where there are many variable factors such as friction and impact.

Regarding the contact state, the passive joint is controlled to be in point contact when the tip of the tweezers touches the table plane. This is because the impact force should be absorbed and the tip of the tweezers move along the plane of the table. In the case tweezers are in a noncontact state except for the fingers, we control the passive joint so that it is in soft-finger contact to achieve stable manipulation. This time, the state of sliding contact is not used for manipulation due to the difficulty of achieving control.

B. Grasping Algorithm

First we explain the common algorithm among three cases, then describe individual algorithms for each case.

The target position in the image plane is defined as $\xi = (u, v)$ and the 3-D position of the target is defined as $\mathbf{x} = (x, y, z)$. Using the perspective projection function \mathbf{f} , we can write $\xi = \mathbf{f}(\mathbf{x})$. From the kinematics of the hand and tweezers structure, we can write the tip of tweezers point as $\mathbf{x} = \mathbf{g}(\mathbf{q})$. The coordinate system is set as shown in Fig.5.

By differentiating this relation,

$$\dot{\xi} = \frac{\partial \mathbf{f}}{\partial \mathbf{x}} \frac{\partial \mathbf{g}}{\partial \mathbf{q}} \dot{\mathbf{q}} \equiv \mathbf{J} \dot{\mathbf{q}} \quad (7)$$

with respect to

$$\dot{\mathbf{q}}_d = \mathbf{J}^+ \left(k(\xi - \xi_d) + \dot{\xi}_d \right), \quad (8)$$

where k is a positive constant and \mathbf{J}^+ means a pseudo inverse matrix of \mathbf{J} . This is resolved-rate control and the

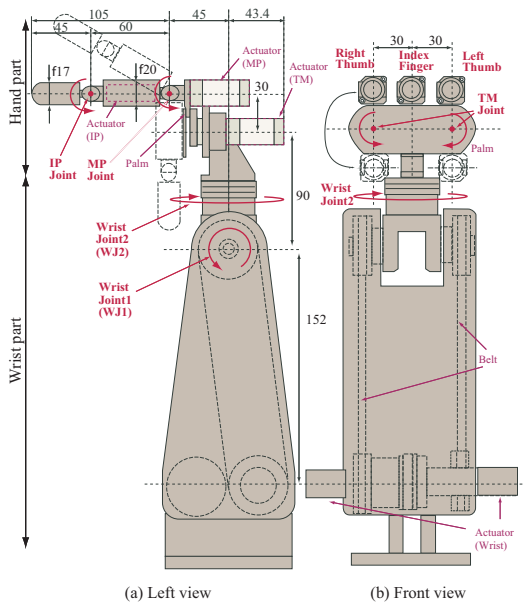


Fig. 7. High-speed hand

following equation is satisfied regarding the error e between desired and actual joint trajectory:

$$\dot{e} + ke = 0. \quad (9)$$

That is, the hand can follow a desired trajectory of the tweezers because the error e converges to zero. Its velocity can be adjusted by the gain k .

1) *Sliding Object on a Plane Surface*: At the moment of impact with a plane, the image Jacobian \mathbf{J} changes in a discontinuous manner because of the transition from soft-finger contact to point contact. Although grasping can be mostly achieved even in such cases because of the robustness of visual servoing, we introduce the following modification in order to improve the success rate:

$$k \rightarrow k + a \left(b - \left| \frac{\partial \xi}{\partial x} \right| \right), \quad (10)$$

where $\frac{\partial \xi}{\partial x}$ means the change rate of image feature and a, b are constant coefficients. It has an effect on the tracking speed of the tweezers for smoother control.

2) *Upward Moving Object in the Air*: In this case, the target velocity gradually decreases because its motion forms a parabola in the air. The hand should not grasp the target immediately after the target is shot upward. Therefore, we set the grasping motion which consists of two phases as shown in Fig.6. Tweezers motion is separated into normal and tangential components because the separation provides intuitive and easy control of the contact state based on the analysis as mentioned in the section II. The hand is controlled in only the u direction in phase I when the target moves fast. This motion can be executed by substituting only the u component of the desired trajectory in image plane. When the velocity of the target is less than a certain threshold, the phase is shifted from I to II. In phase II, the hand is

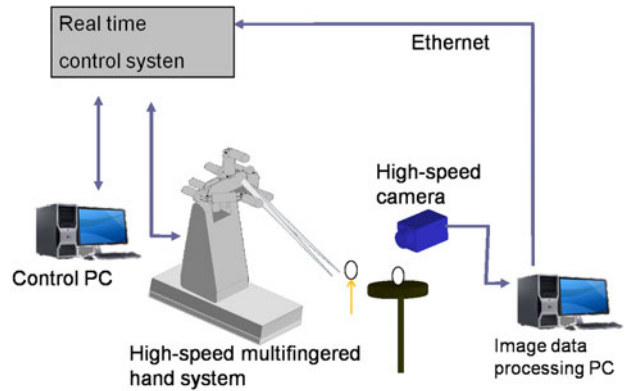


Fig. 8. Experimental system

controlled in both u and v directions, and grasping of the target is completed. This two-stage method has an important role to prevent the state transition from soft-finger contact to point contact caused by excessive inertia force.

3) *Downward Moving Object in the Air*: In this case, the target velocity gradually increases in contrast to the upward moving object. Therefore, the hand is controlled to start grasping motion in all directions immediately after the vision sensor recognizes the target. Moreover the arbitrary constants are modified to set the relative velocity between the tweezers and the target as low as possible. This is because we need to control the hand motion so as not to flip the target at the moment of impact.

IV. EXPERIMENTS

A. System Configuration

The hand consists of three fingers and a wrist as shown in Fig.7. It has 10 degrees-of-freedom (DOF) in total. A small harmonic drive gear and a high-power mini actuator are fitted in each finger link [11]. The design of this actuator is based on the novel concept that maximum power output, rather than rated power output, should be improved. The hand can close its joints at 180 [deg] per 0.1 [s]. Its maximum velocity is 300 [rpm] and the maximum output is 12 [N]. The base of the hand is attached to a slider, which has a 1-DOF translational motion mechanism. The maximum speed of the slider is about 2 [m/s].

The vision system consists of a high-speed camera called Basler A504k. Its resolution is 1280×1024 with 8 bit gray-scale images, and it has a variable frame rate. In the case of full resolution, we can get the images at 500 fps. It is connected to the image processing PC (CPU: Pentium 4, 3.2GHz, Mem: 1.0GB) by cameralink. The image processing PC calculates feature values at 500 fps and send the values to the control processing system (dSPACE) by Ethernet connection.

Figure 8 shows the experimental system.

B. Experimental Setting

We control right and left thumbs to grasp the tweezers and the index finger is not used for manipulation. A plastic

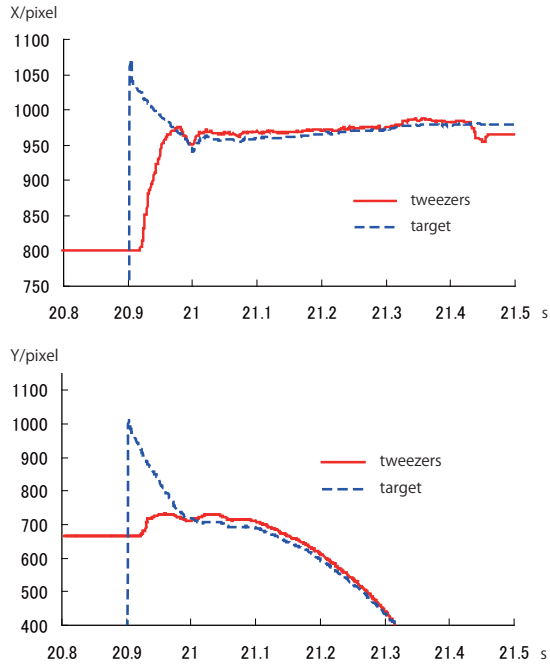


Fig. 9. Motion of tweezers and target in 2D situation

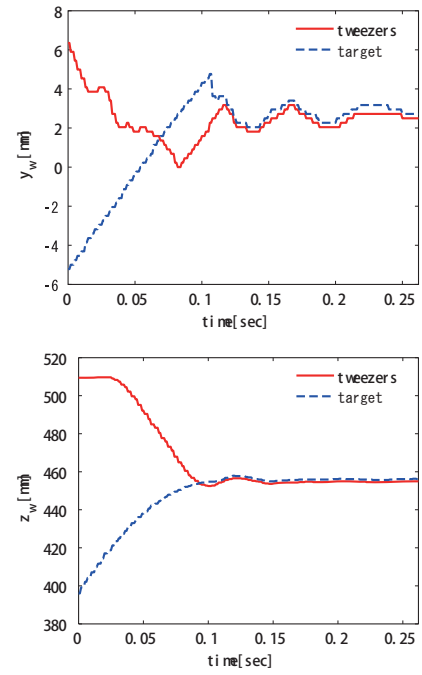


Fig. 10. Motion of tweezers and target in 3D situation

sphere with a radius of 5 [mm] is used as a target. The target is slid on a flat plane toward the hand from front direction in the case (i). The target is released above and below 20 [cm] from the initial height of the tweezers in case (ii) and (iii), respectively. The initial velocity of the target is set as 0.0 [m/s] and 1.1 [m/s] respectively. Silicon rubbers with hardness degrees of $\mu 30$ and $\mu 50$ are used as the flexible material of the fingers.

C. Experimental Result

Figure 9 shows the motion of the target and the tweezers in the image space. The state of the tweezers tips is changed from floating in the air to touching the table plane at $t = 20.93$ and the tweezers tips then move along the surface. The smooth trajectory of the tweezers is generated regardless of the change in state from soft-finger contact to point contact. It turns out that grasping is achieved even for a target moving diagonally to the long axis direction of the tweezers.

Figure 10 shows the motion of the target and the tweezers in y -axis and z -axis direction. First the motion of the tweezers starts to follow the target in only y -axis direction, which means that the state corresponds to the phase I. After 25 [ms], the tweezers follows it in both y -axis and z -axis direction with decrease in velocity of the target. The hand starts to grasp the target at 108 [ms], and then both tweezers and target keep the same motion, which means that grasping of the target is achieved. The vibration in y -axis direction after grasping is caused by impact force acting on elastic elements of tweezers.

Figure 11 shows the continuous photographs every 33 [ms] in the 2D case. Figures 12 and 13 show the continuous photographs every 33 [ms] in the 3D case. In these experiments, the tasks were achieved under the condition that the hand

must grasp the target within 200 [ms] after the vision sensor recognized the target.

The overall success rate was about 40%. Failure was caused mainly by flipping while closing the tweezers. These experimental results are shown as videos on the web-sites [12], [13].

V. CONCLUSIONS

In this paper, we presented an elastic contact model for the design of soft fingers. In addition, the strategy for tweezers control based on high-speed visual servoing was proposed. As a result, grasping of a tiny grain was achieved in 2-D and 3-D situations as examples of tool manipulation.

Our future work will concentrate on detailed analysis of dynamic properties taking advantage of sliding contact and integrate tactile feedback control and high-speed visual servoing. Moreover we plan to achieve various dexterous manipulation with other tools.

REFERENCES

- [1] A. Iriki, M. Tanaka and Y. Iwamura, *Coding of modified body schema during tool use by macaque postcentral neurons*, Neuroreport, Vol.7, No.14, pp.2325-2330, 1996.
- [2] C. Nabeshima, Y. Kuniyoshi and M. Lungarella, *Towards a Model for Tool-Body Assimilation and Adaptive Tool-Use*, Proc. of IEEE Int. Conf. on Development and Learning, pp.288-293, 2007.
- [3] Y. Shinchi and T. Nagai, *A Model of Tools Usage Based on Visual Observation*, IEICE Technical Report, SIS-107(548), pp.27-32, 2008.
- [4] J. H. Connell and M. Brady, *Generating and Generalizing Models of Visual Objects*, Artificial Intelligence, Vol.31, No.2, pp.159-183, 1987.
- [5] Y. Hattori, K. Kise, T. Kitahashi and K. Fukunaga, *Recognition of Functions of Objects Based on Models of Dynamic Functions*, IPSJ Journal, Vol.36, No.10, pp.2277-2285, 1995.
- [6] E. Rivlin, S. J. Dickinson and A. Rosenfeld, *Recognition by Functional Parts*, Proc. of Computer Vision and Pattern Recognition, pp.267-274, 1994.

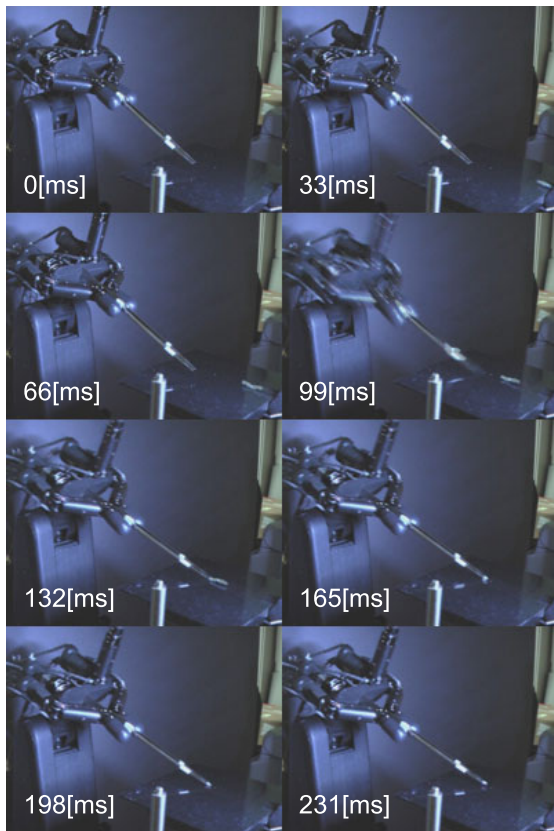


Fig. 11. Hand motion for sliding object

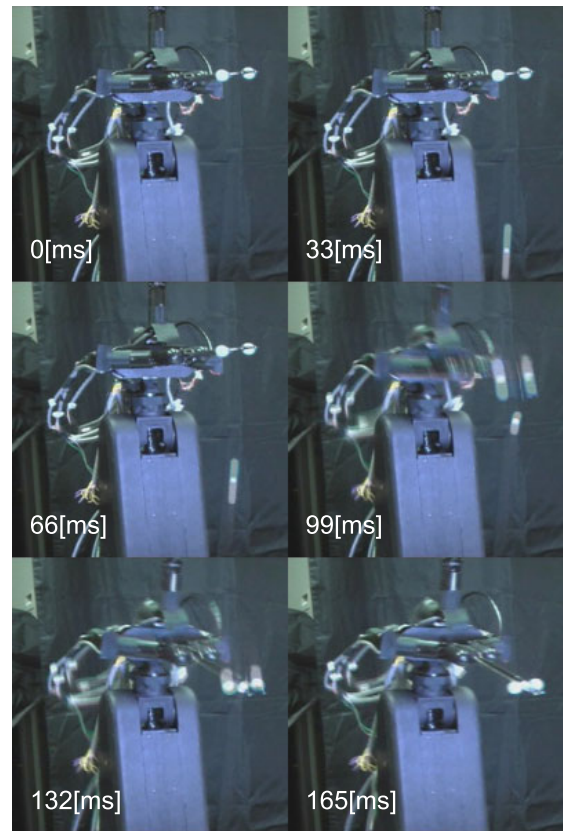


Fig. 12. Hand motion for upward moving object

- [7] H. Sugiuchi and T. Morino, *A Pair of Scissors Handling Task with Dual Multi-Finger Hand Arm System Add vision support functions*, JSME Conference on Robotics and Mechatronics, pp.D6(1)-2A1, 2003.
- [8] H. Kawasaki, T. Mouri, S. Ikenohata, Y. Ohtsuka and T. Endo, *Multi-Fingered Haptic Interface Robot Handling Plural Tool Devices*, Proc. of Second Joint EuroHaptics Conference and Symposium on Haptic Interfaces for Virtual Environment and Teleoperator Systems, pp.397-402, 2007.
- [9] K. Bernardin, K. Ogawara, K. Ikeuchi and R. Dillmann, *A Sensor Fusion Approach for Recognizing Continuous Human Grasping Sequences Using Hidden Markov Models*, IEEE Transactions on Robotics, Vol.21, No.1, pp 47-57, 2005.
- [10] S. Mizusawa, A. Namiki and M. Ishikawa, *Tweezers Type Tool Manipulation by a Multifingered Hand Using a High-Speed Visual Servoing*, Proc. of IEEE/RSJ Int. Conf. on Intelligent Robots and Systems, pp.2709-2714, 2008.
- [11] A. Namiki, Y. Imai, M. Ishikawa and M. Kaneko, *Development of a High-speed Multifingered Hand System and Its Application to Catching*, IEEE/RSJ Proc. of Int. Conf. on Intelligent Robots and Systems, pp.2666-2671, 2003.
- [12] http://www.k2.t.u-tokyo.ac.jp/fusion/tool_manipulation/
- [13] <http://www.k2.t.u-tokyo.ac.jp/fusion/TweezersCatching/>

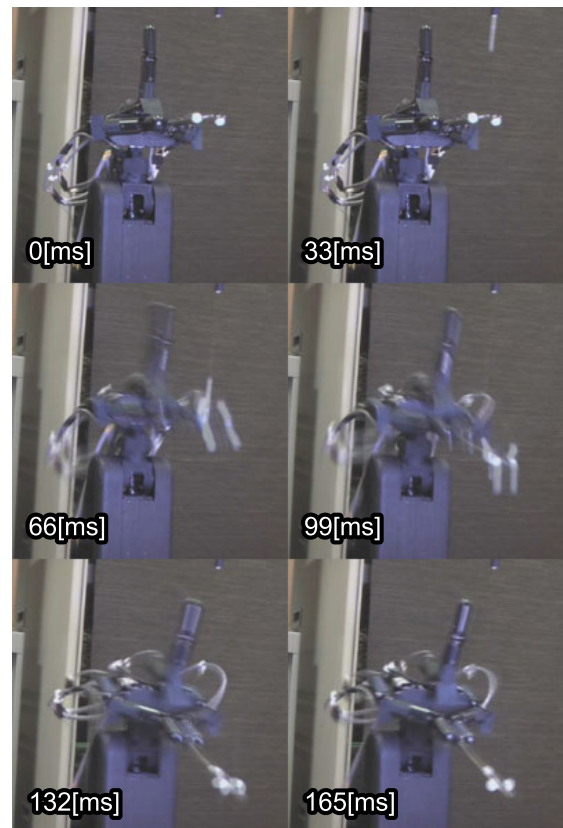


Fig. 13. Hand motion for downward moving object